International Journal of Thermophysics, Vol. 25, No. 5, September 2004 (© 2004)

Viscosity and Surface Tension of Saturated *n*-Pentane[1]

A. P. Fröba,[2,3] L. Penedo Pellegrino,[4] and A. Leipertz[2]

Light scattering by thermally excited capillary waves on liquid surfaces or interfaces can be used for the investigation of viscoelastic properties of fluids. In this work, the simultaneous determination of surface tension and liquid kinematic viscosity of *n*-pentane by surface light scattering (SLS) on a gas–liquid interface was carried out. The experiments are based on a heterodyne detection scheme and signal analysis by photon correlation spectroscopy (PCS). Measurements were performed under saturation conditions over a wide temperature range from about 233 to 363 K. For the whole temperature range the total uncertainty of the liquid kinematic viscosity and surface tension is estimated to be better than 1.0 and 1.2%, respectively. The results obtained corroborate the reliability of the SLS technique for the determination of thermophysical properties.

KEY WORDS: dynamic light scattering; *n*-pentane; surface light scattering; surface tension; viscosity.

1. INTRODUCTION

In the present work we carried out the simultaneous determination of the liquid kinematic viscosity and surface tension of *n*-pentane by surface light scattering (SLS), a technique which is closely related to dynamic light scattering (DLS) in its classical form. The difference is that this technique probes, as the name indicates, fluctuations on the surface of a liquid or,

[1]Paper presented at the 15th Symposium on Thermophysical Properties, June 22–27, 2003, Boulder, Colorado, U.S.A.

[2]Lehrstuhl für Technische Thermodynamik (LTT), Friedrich-Alexander-Universität Erlangen-Nürnberg, Am Weichselgarten 8, D-91058 Erlangen, Germany.

[3]To whom correspondence should be addressed. E-mail: apf@ltt.uni-erlangen.de

[4]Departamento de Química e Bioquímica, Faculdade de Ciências da Universidade de Lisboa, Campo Grande, Edifício C8, 1749-016 Lisboa, Portugal.

0195-928X/04/0900-1323/0

in a more general formulation, at phase boundaries. The present investigations for *n*-pentane were initiated by recent research activities of the International Association for Transport Properties (IATP). Here, the aim was to get a comprehensive and reliable database for the viscosity of *n*-pentane which has been proposed as a possible standard for the low-viscosity region. Especially, because of the lack of reference data for the liquid viscosity of *n*-pentane under true saturation conditions, the need for further experimental investigations was established.

In the following, at first the methodological principles of SLS for the determination of viscosity and surface tension are briefly reviewed. For a more detailed and comprehensive description of the underlying theory, the reader is referred to the specialized literature [1–4]. After a description of our SLS apparatus, which allows in the case of transparent fluids, as is of interest to this work, the analysis of scattered light in the forward direction, the experimental results for surface tension and liquid kinematic viscosity of saturated *n*-pentane are presented and discussed in comparison with literature results.

2. METHOD

Liquid–vapor interfaces in macroscopic thermal equilibrium exhibit surface waves which are caused by the thermal movement of molecules and which are quantized in so-called "ripplons" [5]. In general, for the temporal decay of surface fluctuations two cases may be distinguished [6]. In the case of large viscosity and/or small surface tension, the amplitude of surface waves is damped exponentially. For small viscosities, as is relevant in the experiments described here, the amplitude of surface waves decays in the form of a damped oscillation. SLS analyzes the light scattered by surface waves. Each of these fluctuations behaves optically as a weak phase grating and scatters a small fraction of the incident light in equally spaced directions around both the reflected and refracted beams.

With the light scattering geometry used in this work, scattered light is observed in the forward direction near refraction; see Fig. 1. This arrangement has been chosen due to signal and stability considerations [7] and differs from the more commonly employed scattering geometry where the scattered light is observed close to the direction of the reflected beam. By the choice of the angle of incidence ε, resulting in a specific angle δ of the refracted light, and the scattering angle Θ_S, the scattering vector $\vec{q} = \vec{k}'_I - \vec{k}'_S$ is determined, and from this, the wave vector and frequency of the observed surface vibration mode. Here, $\vec{k}'_I$ and $\vec{k}'_S$ denote the projections of the wave vectors of the refracted ($\vec{k}_I$) and scattered light ($\vec{k}_S$)

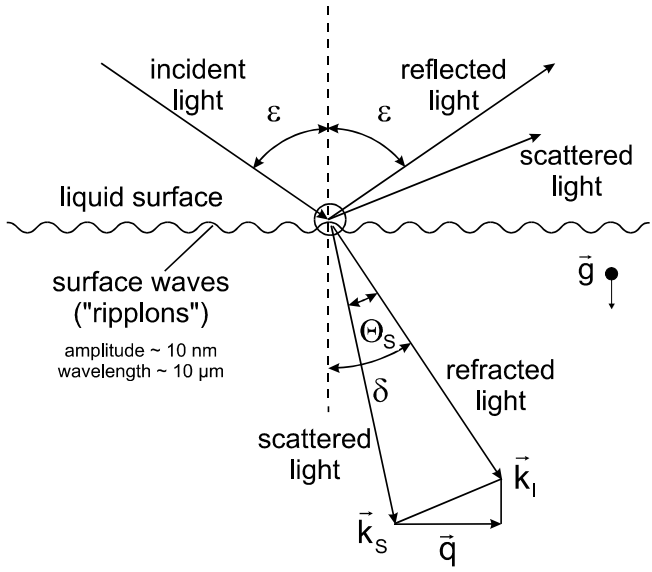

Fig. 1. Scattering geometry: light scattering by surface waves.

in the surface plane, respectively. For the observation of scattered light within the irradiation plane and assuming elastic scattering (i.e., $k_I \cong k_S$), the modulus of the scattering vector is expressed by

$$\begin{aligned} q &= \left|\vec{k}'_I - \vec{k}'_S\right| \cong 2k_I \sin(\Theta_S/2)\cos(\delta - \Theta_S/2) \\ &= \frac{4\pi n}{\lambda_0}\sin(\Theta_S/2)\cos(\delta - \Theta_S/2), \end{aligned} \tag{1}$$

where n is the fluid refractive index and λ_0 is the laser wavelength in vacuo.

In light scattering experiments the surface fluctuations result in a temporal modulation of the scattered light intensity. Information about the dynamics of surface waves, i.e., their frequency and damping, can be derived through a temporal analysis of the scattered light intensity by using photon correlation spectroscopy (PCS). In the case of large heterodyning where the scattered light is superimposed with stronger coherent reference light, the time-dependent intensity correlation function for the analysis of surface fluctuations is described by [8]

$$G^{(2)}(\tau) = A + B\cos(\omega_R|\tau| - \phi)\exp(-|\tau|/\tau_C), \tag{2}$$

assuming the decay of the amplitude of surface waves is oscillatory. The experimental constants A and B are essentially determined by the total number of counts registered, the ratio of scattered light to reference light, and the coherence properties of the optical system. The phase term ϕ, $\phi = \text{atan}(\Gamma/\omega_R)$, largely accounts for the deviations of the power spectrum of the surface fluctuations from the Lorentzian form, and the correlation time τ_C and the frequency ω_R are identical with the mean lifetime or the reciprocal of the damping constant Γ $(=1/\tau_C)$ of "ripplons" and the frequency of propagation, respectively. The latter relate to the fluid properties of the liquid–vapor interface through the surface wave dispersion equation [9, 10],

$$\left\{\left[i\alpha(\eta' m' + \eta' q + \eta'' m'' + \eta'' q)\right]\left[\sigma q^2 + i\alpha(\eta' m' + \eta' q + \eta'' m'' + \eta'' q) + g(\rho' - \rho'') - \frac{\alpha^2}{q}(\rho' + \rho'')\right] - \left[i\alpha(\eta' q - \eta' m' + \eta'' m'' - \eta'' q)\right]^2\right\} = 0, \tag{3}$$

where

$$\alpha = \omega_R + i\Gamma, \tag{4}$$

$$m' = \sqrt{q^2 + i\frac{\alpha\rho'}{\eta'}}, \qquad m'' = \sqrt{q^2 + i\frac{\alpha\rho''}{\eta''}}, \tag{5}$$

g is the acceleration of gravity, σ the surface tension, ρ' and ρ'' are the densities of the liquid and vapor phases, respectively, and η' and η'' are the dynamic viscosities of the liquid and vapor phases, respectively. This complex relation is the result of the solution of the linearized Navier–Stokes equation whereby the fluid flow must satisfy boundary conditions that express the continuity of normal and tangential stresses at the liquid–vapor interface [2].

To a first-order approximation, the ratio of the sum of the dynamic viscosities of the liquid and vapor phase relative to the sum of the densities of the liquid and vapor phase may be obtained from the decay time τ_C of the correlation function Eq. (2) by

$$\frac{\eta' + \eta''}{\rho' + \rho''} \approx \frac{1}{2\tau_C q^2}. \tag{6}$$

Furthermore, the correlation function Eq. (2) can simultaneously be evaluated for the ratio of the surface tension to the sum of the densities of the vapor and liquid phases,

$$\frac{\sigma}{\rho' + \rho''} \approx \frac{\omega_R^2}{q^3}, \tag{7}$$

which, to a first-order approximation, follows directly from the beat frequency ω_R and the modulus of the wave vector q.

For a reliable determination of viscosity and surface tension, a more detailed and rigorous consideration of the SLS method than given by Eqs. (6) and (7) must be applied. In the present work, however, data for the liquid kinematic viscosity and surface tension were obtained by an exact numerical solution of the dispersion equation for surface waves at a liquid–vapor interface, Eq. (3), where the measured frequency ω_R, the damping Γ, and the modulus of the wave vector q are used as input values.

3. EXPERIMENTAL

The experimental setup used for the investigation of a liquid–vapor interface of *n*-pentane under saturation conditions is shown in Fig. 2. A frequency-doubled continuous-wave Nd:YVO_4-laser operated in a single mode with a wavelength of $\lambda_0 = 532$ nm serves as a light source. The laser power was about 200 mW when working at temperatures $T < 300$ K and somewhat lower for higher temperatures. For the observation of light scattered by surface waves, the optical path has to be aligned in such a way that the laser beam and the direction of detection intersect on the liquid–vapor interface in the measurement cell. For large scattering intensities from the vapor–liquid interface, scattered reference light from the cell windows is not sufficient to realize heterodyne conditions. Here, an additional reference beam is added. To this end, part of the incident laser light is split by a glass plate and superimposed with the scattered light behind the sample cell. The time-dependent intensity of the scattered light is detected by two photomultiplier tubes (PMTs) operated in cross-correlation in order to suppress after-pulsing effects. The signals are amplified, discriminated, and fed to a digital correlator with 256 linearly spaced channels operated with a sample time down to 40 ns.

The main feature of the optical arrangement, however, is based on the analysis of scattered light at variable and relatively high wave numbers of capillary waves, whereby instrumental broadening effects are negligible [3]. Light scattered on the liquid–vapor interface of *n*-pentane is detected perpendicular to the surface plane, which means $\Theta_S = \delta$, see Fig. 1. For this arrangement, with the help of Snell's refraction law and simple trigonometric identities, the modulus of the scattering vector q can be deduced as a function of the easily accessible angle of incidence,

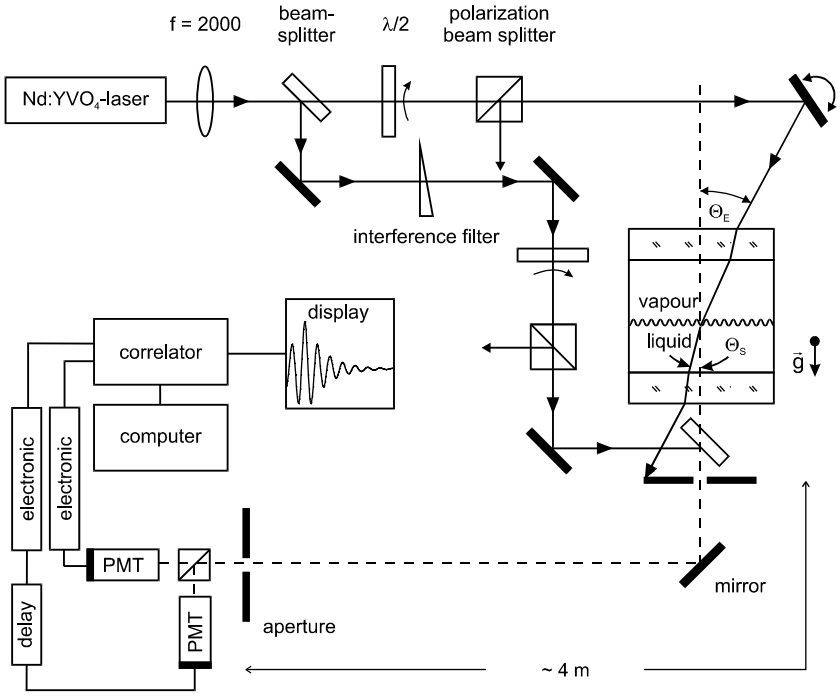

Fig. 2. Experimental setup: optical and electronic arrangement.

$$q = \frac{2\pi}{\lambda_0} \sin(\Theta_E). \tag{8}$$

For measurement of the angle of incidence Θ_E, the laser beam is first adjusted through the detection system consisting of two apertures (Ø1–2 mm) at a distance of about 4 m. Then the laser beam is set to the desired angle which for the experiment was between 3.0° and 4.0° and was measured with a high precision rotation table. The error in the angle measurement has been determined to be approximately ±0.005°, which results in a maximum uncertainty of less than 1% for the desired thermophysical properties.

According to the specification of the manufacturer (Merck GmbH, Darmstadt), the *n*-pentane sample was of spectroscopic grade (Uvasol®) with a minimum purity of 99.5% and was used without further purification. For the present measurements, the sample was filled from the liquid phase into an evacuated cylindrical pressure vessel (diameter, 70 mm; volume, 150 cm^3) equipped with two quartz windows (Herasil I; diameter, 30 mm; thickness, 30 mm). The temperature regulation of the cell surrounded by an

insulating housing was realized with electrical heating. For temperatures below room temperature, the insulating housing was cooled to about 10 K below the desired temperature in the sample cell using a lab thermostat. The temperature of the cell was measured with two calibrated Pt-100 Ω resistance probes, integrated into the main body of the vessel, with a resolution of 0.25 mK using an ac bridge (Paar, MKT 100). The uncertainty of the absolute temperature measurement was better than ±0.015 K. The temperature stability during an experimental run was better than ±0.001 K. For each temperature, at least eight measurements at different angles of incidence were performed, where the laser was irradiated from either side with respect to the axis of observation in order to check for possible misalignment. The measurement times for a single run were typically of the order of 10 min down to 5 min for the highest temperatures in this study.

4. RESULTS AND DISCUSSION

4.1. Measurement Data and Uncertainty

The results for the liquid kinematic viscosity and surface tension of *n*-pentane under saturation conditions from surface light scattering are summarized in Table I. The listed data are average values of at least eight independent measurements with different angles of incidence Θ_E. Also listed in Table I are the values from the literature used for data evaluation as described below.

Data obtained from surface light scattering for the dynamics of surface waves, i.e., frequency ω_R and damping Γ $(=1/\tau_C)$ at a defined wave vector q, have been combined with reference data for the dynamic viscosity of the vapor phase η'' and density data for both phases ρ' and ρ'' to get information about the liquid kinematic viscosity ν' and surface tension σ, see Section 2, Eq. (3). Both liquid and vapor densities have been adopted from a multiparameter equation of state of Span and Wagner [11]. Data for the dynamic viscosity of the vapor phase have been calculated according to a method given in Refs. 12 and 13.

Taking into account the uncertainties of the individual quantities entering into the calculation, the uncertainty of our liquid kinematic viscosity data is estimated to be better than 1% for the whole temperature range investigated in the course of this work. It should be noted that even approximate values for the dynamic viscosity of the vapor phase are sufficient to achieve such an accuracy. For the existing surface tension data, the uncertainty is estimated to be better than 1.2%. A more detailed discussion regarding the accuracy achievable for liquid kinematic viscosity and surface tension from SLS can be found in Refs. 3 and 4.

Table I. Liquid Kinematic Viscosity ν' and Surface Tension σ of *n*-Pentane Under Saturation Conditions[a]

T (K)	$\eta''(\mu\text{Pa}\cdot\text{s})$	$\rho'(\text{kg}\cdot\text{m}^{-3})$	$\rho''(\text{kg}\cdot\text{m}^{-3})$	$\nu'(\text{mm}^2\cdot\text{s}^{-1})$	$\sigma(\text{mN}\cdot\text{m}^{-1})$
233.15	5.38	681.54	0.10	0.6423	22.61
243.15	5.60	672.57	0.18	0.5790	21.39
253.15	5.83	663.47	0.31	0.5263	20.28
263.15	6.08	654.23	0.51	0.4796	19.16
273.15	6.33	644.86	0.79	0.4413	18.16
283.15	6.59	635.35	1.19	0.4102	17.03
293.15	6.86	625.67	1.73	0.3782	15.82
303.15	7.13	615.80	2.44	0.3516	14.73
313.15	7.40	605.69	3.37	0.3252	13.66
323.15	7.67	595.32	4.55	0.3047	12.53
333.15	7.95	584.62	6.04	0.2818	11.53
343.15	8.22	573.55	7.89	0.2625	10.52
353.15	8.49	562.03	10.15	0.2449	9.41
363.15	8.77	550.00	12.91	0.2283	8.44

[a] Directly measured values for frequency ω_R and damping Γ at a defined wave vector q of surface waves were combined with theoretically calculated values for η'' and data for ρ' and ρ'' from Ref. 11 to derive ν' and σ by an exact numerical solution of the dispersion relation Eq. (3).

4.2. Data Correlation

For the complete temperature range studied in the present investigation, a modified Andrade-type equation which in its simple form is commonly chosen to represent the dynamic viscosity at least over a limited temperature range was used in the form,

$$\nu' = \nu'_0 \exp[\nu'_1 T^{-1} + \nu'_2 T + \nu'_3 T^{-2}] \tag{9}$$

in order to represent our experimental kinematic viscosity data for *n*-pentane, where T is the temperature in K and the coefficients are given in Table II. Here, also the standard deviation (rms) of our data relative to those calculated by Eq. (9) is reported. It should be noted that the residuals of the experimental data from the fit are smaller than the standard deviations of the individual measurements which were in all cases smaller than $\pm 1.0\%$.

The experimental data for the surface tension can well be represented by a modified van der Waals-type surface tension equation of the form [14],

$$\sigma = \sigma_0 (1 - T_R)^{1.26} \left[1 + \sigma_1 (1 - T_R)^{0.5} + \sigma_2 (1 - T_R) \right], \tag{10}$$

Table II. Coefficients of Eq. (9)

ν_0' ($mm^2 \cdot s^{-1}$)	340.58
ν_1' (K)	−1608.14
ν_2' (K^{-1})	−0.0117528
ν_3' (K^2)	182897
rms (%)	0.23
T-range (K)	233–363

where the fit parameters σ_0, σ_1, and σ_2 are given in Table III. In Eq. (10) $T_R = T/T_C$ represents the reduced temperature, where T is the absolute temperature and T_C is the critical temperature. For the latter a value of 469.70 K was adopted from the corresponding reference [11] used to get information about the vapor and liquid densities under saturation conditions. The present correlation represents the experimental values of the surface tension with a root-mean-square deviation of about 0.3%.

4.3. Comparisons with Literature Data

4.3.1. Kinematic Viscosity

In Fig. 3 the kinematic viscosity of *n*-pentane under saturation conditions has been plotted in comparison with literature data in the upper part. In the lower part of Fig. 3 the deviations between the correlation Eq. (9) obtained with our experimental results and the data of other research groups are shown. Liquid viscosity values at true saturation conditions obtained with a capillary viscometer by Golubev [15] and Golubev and Agaev [16] have been included in Fig. 3. Since most experimental data available in the literature are concerned with high pressure conditions in the compressed liquid state, see, e.g., Refs. 17–21, we made for these data sets an extrapolation or interpolation of viscosity isotherms to be able to perform a data comparison for saturation conditions. For the

Table III. Coefficients of Eq. (10)

σ_0 ($mN \cdot m^{-1}$)	45.32
σ_1	0.779
σ_2	–0.737
rms (%)	0.29
T-range (K)	253–363

measurements by Oliveira and Wakekam [17] which were performed along two isotherms at 303.15 and 323.15 K for pressures up to about 250 MPa with a vibrating-wire viscometer, an uncertainty of ±0.5% is stated. In the same paper for the pressure dependence of the viscosity of *n*-pentane, correlations in the form of polynomials were presented which have been extrapolated to the vapor pressure in the course of this work to obtain values at saturation conditions. Kiran and Sen [18] measured the viscosity of *n*-pentane with a specially designed falling-cylinder viscometer in a pressure range from 10 to 70 MPa at temperatures from 310 to 450 K. In Ref. 18 an exponential relationship was used to describe the density dependence of the viscosity which has been extrapolated to the saturated liquid density for data comparisons. Measurements of Reamer et al. [19] were performed with a rotating-cylinder viscometer, at pressures up to about 35 MPa and at temperatures of 310.9, 344.3, 377.6, and 410.9 K. Reamer et al. [19] have reported for their experimental values relative to those calculated by their own correlations a standard error of 0.75%. Also shown in Fig. 3 are measurements by Hubbard and Brown [20], Sage and Lacey [21], and Estrada-Baltazar et al. [22] which were performed by a rolling-ball viscometer. While the data of Hubbard and Brown [20] and Sage and Lacey [21] were extrapolated to saturation conditions as given in Ref. 19, the single data point from the work of Estrada-Baltazar et al. [22] was taken at atmospheric pressure. Additionally included in Fig. 3 are data from a prediction method by Assael et al. [23] which is based on the hard-sphere theory whereby experimental data obtained by the same authors with a vibrating wire viscometer for pressures up to 70 MPa for some *n*-alkanes have been used for an improved correlation scheme. Finally, for the liquid kinematic viscosity of saturated *n*-pentane, calculated data from the NIST reference database [24] and the work of Lee et al. [25] have been included in Fig. 3. For the latter the viscosity behavior of *n*-pentane is described by a nine-parameter equation by simply inserting its molecular weight and density values and without any knowledge of experimental *n*-pentane viscosity data [26].

For the conversion of data from dynamic to kinematic viscosity, density data from the multiparameter equation of state by Span and Wagner [11] have been used. Furthermore, density data from the same work were used for the calculation of the correlation or prediction schemes given in Refs. 18, 23, and 25. Good agreement can be found between the data of Sage and Lacey [21] and our results, the maximum deviation is 1.9%. Within the temperature ranges from 263 to 303 K and 333 to 373 K, our viscosity data for *n*-pentane agree with the experimental data sets of Golubev [15] and Golubev and Aagaev [16], respectively. Other references based on experimental data show systematic deviations up to ±7.5%, see

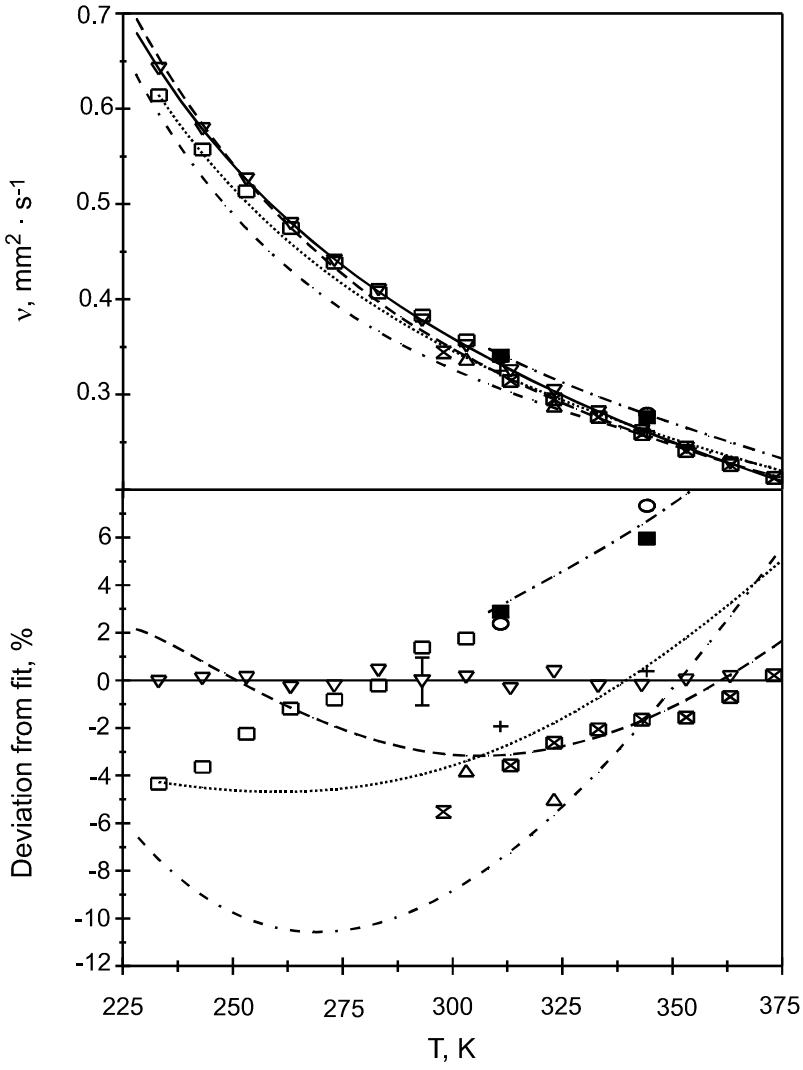

Fig. 3. Kinematic viscosity of liquid *n*-pentane under saturation conditions from SLS in comparison with literature data. ∇ ——, this work; ⊠, Golubev [15]; □, Golubev and Agaev [16]; Δ, Oliveira and Wakeham [17]; ---, Kiran and Sen [18]; ■, Reamer et al. [19]; ○, Hubbard and Brown [20]; —+—, Sage and Lacey [21]; ⧖, Estrada-Baltazar et al. [22]; ——·, Assael et al. [23]; ·····, NIST reference database [24]; ——, Lee et al. [25].

Ref. 20, and even larger ones for the extrapolated data set of Kiran and Sen [18]. An explanation for this behavior could be the use of extrapolated values instead of values obtained under the same experimental conditions. While for the whole temperature range the agreement between our data correlation and the predictions given by Lee et al. [25] can be regarded to be satisfactory, with deviations smaller than 3%, large differences of up to −10.6% can be found for the prediction scheme by Assael et al. [23] which is based on the hard-sphere theory. The literature data show, however, significant differences between themselves as can be seen in the deviation plot.

4.3.2. Surface Tension

Surface tension data and deviations from our correlation function Eq. (10) are displayed in Fig. 4. Comparisons with literature data are also performed for *n*-pentane under saturation conditions between 225 and 375 K. The measurements by Jasper and Kring [27] were performed under isobaric conditions at 0.1 MPa in a temperature range between 273.15 and 303.15 K in an atmosphere containing dry nitrogen and the vapor phase of the hydrocarbon. Jasper and Kring [27] used a specially designed capillary meter to measure the surface tension at a relatively small volume of liquid. Grigoryev et al. [28] have obtained the surface tension of *n*-pentane under saturation conditions with the differential capillary-rise method for temperatures between the triple point and the critical point. In addition to the measured values, the correlation from Ref. 28 is shown based on a two-term modified van der Waals-type surface-tension equation. Here, a standard deviation of the fit to surface tension data of 0.18 $mN \cdot m^{-1}$ is stated. For data comparisons, Fig. 4 also includes a three-parameter generalized equation as proposed by Somayajulu [29] for data correlation of the surface tension from the triple point to the critical point. With this type of regression surface tension data available for *n*-pentane in the literature are represented with an average deviation of 0.025 $mN \cdot m^{-1}$. Furthermore, an extended scaled equation for the temperature dependence of the surface tension as proposed by Miqueu et al. [14] for several pure fluids is compared in Fig. 4. This prediction yields values of the surface tension within an average of 3.5% of the measured values for all compounds studied in Ref. 14. A correlation scheme given by Romero-Martinez and Trejo [30] for the surface tension of homologous series of pure liquid hydrocarbons, as a function of molecular weight and temperature, based on the work of Grigoryev et al. [28] is also presented in Fig. 4. The standard deviation obtained in the work of Romero-Martinez and Trejo [30] from the correlation of 94 experimental points was 0.16 $mN \cdot m^{-1}$. Finally, values from the data compilation of Vargaftik [31] are included in Fig. 4.

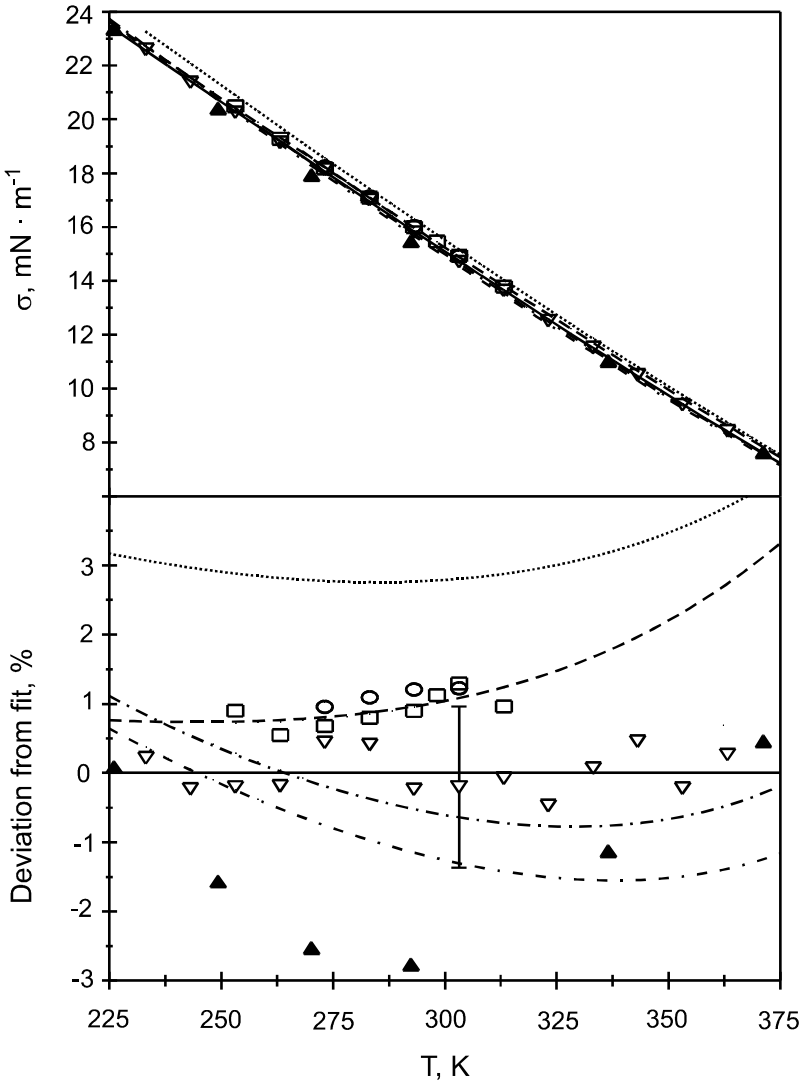

Fig. 4. Surface tension of *n*-pentane under saturation conditions from SLS in comparison with literature data. ▽—, this work; ∘, Jasper and Kring [27]; ▲ – –·, Grigoryev et al. [28]; ––, Somayajulu [29]; · · · · · · ·, Miqueu et al. [14]; – · –, Romero-Martínez and Trejo [30]; □, Vargaftik [31].

As can be seen in the deviation plot of Fig. 4, the maximum difference between our correlation and the literature data is less than ±4%. A maximum deviation between +3 and +4% is found for comparisons of our data with the extended scaled equation of Miqueu et al. [14]. The

maximum deviations of the experimental data from Ref. 28 and 27 are slightly below 3% and above 1%, respectively. Correlations from Grigoryev [28] and Romero-Martínez and Trejo [30] show very good agreement with our fit. In this case the deviation has about the same magnitude as the uncertainty of our experimental data, which is about 1%.

5. CONCLUSIONS

Experimental values of the liquid kinematic viscosity and surface tension of *n*-pentane from SLS have been presented. Measurements have been performed under true saturation conditions over a temperature range from 233 to 363 K. For data evaluation a correct theoretical treatment of the capillary-wave problem for a liquid–vapor interface has been applied. With the help of reference data for the liquid and vapor densities and calculated data for the dynamic viscosity of the vapor phase – yet without any calibration procedure – an overall uncertainty of 1% and 1.2% could be achieved for the liquid kinematic viscosity and surface tension, respectively. For the surface tension agreement with literature data can be considered to be satisfactory. For the viscosity of *n*-pentane comparisons with reference data covering the past century result in large differences of up to 8%. An improvement of the situation for the viscosity of saturated *n*-pentane requires more accurate measurements under well defined conditions.

REFERENCES

1. D. Langevin, *Light Scattering by Liquid Surfaces and Complementary Techniques* (Marcel Dekker, New York, 1992).
2. E. H. Lucassen-Reynders and J. Lucassen, *Advan. Colloid Interface Sci.* **2**:347 (1969).
3. A. P. Fröba, *Simultane Bestimmung von Viskosität und Oberflächenspannung transparenter Fluide mittels Oberflächenlichtstreuung*, Dr.-Ing. thesis (Friedrich-Alexander-Universität Erlangen-Nürnberg, Erlangen 2002).
4. A. P. Fröba and A. Leipertz, *Int. J. Thermophys.* **24**:895 (2003).
5. W. Brouwer and R. K. Pathria, *Phys. Rev.* **163**:200 (1967).
6. R. H. Katyl and U. Ingard, *Phys. Rev. Lett.* **19**:64 (1967).
7. K. Sakai, P.-K. Choi, H. Tanaka, and K. Takagi, *Rev. Sci. Instrum.* **62**:1192 (1991).
8. E. S. Wu and W. W. Webb, *Phys. Rev. A* **8**:2077 (1973).
9. P. M. Papoular, *J. de Phys. (Paris)* **29**:81 (1968).
10. J. Meunier, *J. de Phys. (Paris)* **30**:933 (1969).
11. R. Span and W. Wagner, *Int. J. Thermophys.* **24**:41 (2003).
12. K. Lucas, *C. I. T.* **46**:157 (1974).
13. R. C. Reid, J. M. Prausnitz, and B. E. Poling, *The Properties of Gases and Liquids* (McGraw-Hill, New York, 1977, 1987).

14. C. Miqueu, D. Broseta, J. Satherley, B. Mendiboure, J. Lachaise, and A. Graciaa, *Fluid Phase Equilib*. **172**:169 (2000).
15. I. F. Golubev, *Viscosity of Gases and Gas Mixtures* (Fizmat Press, Moscow, 1959).
16. I. F. Golubev and N. A. Agaev, *Viscosity of Limiting Hydrocarbons*, (Azerbaydzhan State Press, Baku, 1964).
17. C. M. B. P. Oliveira and W. A. Wakeham, *Int. J. Thermophys*. **13**:773 (1992).
18. E. Kiran and Y. L. Sen, *Int. J. Thermophys*. **13**:411 (1992).
19. H. H. Reamer, G. Cokelet, and B. H. Sage, *Anal. Chem*. **31**:1422 (1959).
20. R. M. Hubbard and G. G. Brown, *Ibid*. **35**:1276 (1943).
21. B. H. Sage and W. N. Lacey, *Trans. Am. Inst. Mining Met. Engrs*. **127**:118 (1938).
22. A. Estrada-Baltazar, G. A. Iglesias-Silva, and M. A. Barrufet, *J. Chem. Eng. Data* **43**:601 (1998).
23. M. J. Assael, J. H. Dymond, M. Papadaki, and P. M. Patterson, *Int. J. Thermophys*. **13**:269 (1992).
24. *Standard Reference Database 14*, Version 4, National Institute of Standards Technology (NIST), Boulder, Colorado (2000).
25. A. L. Lee, K. E. Starling, J. P. Dolan, and R. T. Ellington, *AIChE J*. **10**:694 (1964).
26. A. L. Lee and R. T. Ellington, *J. Chem. Eng. Data* **10**:101 (1965).
27. J. J. Jasper and E. Kring, *J. Phys. Chem*. **59**:1019 (1955).
28. B. A. Grigoryev, B. V. Nemzer, D. S. Kurumov, and J. V. Sengers, *Int. J. Thermophys*. **13**:453 (1992).
29. G. R. Somayajulu, *Int. J. Thermophys*. **9**:559 (1988).
30. A. Romero-Martínez and A. Trejo, *Int. J. Thermophys*. **19**:1605 (1998).
31. N. B. Vargaftik, *Tables on the Thermophysical Properties of Liquids and Gases in Normal and Dissociated States* (Hemisphere, Washington, D.C., 1983).